Actinorhodin Biosynthesis: Structural Requirements for Post-PKS Tailoring Intermediates Revealed by Functional Analysis of ActVI-ORF1 Reductase†

Takayuki Itoh,‡ Takaaki Taguchi,§ Meriel R. Kimberley,|| Kevin I. Booker-Milburn,|| G. Richard Stephenson,⊥ Yutaka Ebizuka,‡ and Koji Ichinose*,§

Graduate School of Pharmaceutical Sciences, The University of Tokyo, Hongo, Bunkyo-ku, Tokyo 113-0033, Japan, Research Institute of Pharmaceutical Sciences, Musashino University, Shinmachi, Nishitokyo-shi, Tokyo 202-8585, Japan, School of Chemistry, University of Bristol, Cantock's Close, Bristol BS81TS, U.K., and School of Chemical Sciences and Pharmacy, University of East Anglia, Norwich NR4 7TJ, U.K.

Received January 30, 2007; Revised Manuscript Received April 25, 2007

ABSTRACT: Actinorhodin (ACT) produced by *Streptomyces coelicolor* A3(2) is an aromatic polyketide antibiotic, whose basic carbon skeleton is derived from type II polyketide synthase (PKS). Although an acyl carrier protein (ACP) serves as an anchor of nascent intermediates during chain elongation in the type II PKS complex, it generally remains unknown when an ACP-free intermediate is released from the complex to post-PKS modification ("tailoring") steps. In ACT biosynthesis, a stereospecific ketoreductase (RED1) encoded by *act*VI-ORF1 reduces the 3β-keto group of a proposed bicyclic intermediate to an (*S*) secondary alcohol. The bicyclic intermediate is formed from the steps of PKS and its closely associated enzymes and lies at the interface toward ACT-tailoring steps. To clarify whether RED1 recognizes the ACP-bound bicyclic intermediate or the ACP-free bicyclic intermediate, recombinant RED1 was purified for enzymatic characterization. RED1 was heterologously expressed in *Escherichia coli* and purified using Ni-chelate and gel filtration column chromatographies to homogeneity in soluble form. Enzymatic studies *in vitro* on RED1 with synthetic analogues, in place of an unstable bicyclic intermediate, showed that RED1 recognizes 3-oxo-4-naphthylbutyric acid (ONBA) as a preferred substrate and not its *N*-acetylcysteamine thioester. This strongly suggests that RED1 recognizes ACP-free bicyclic β-keto acid as the first committed intermediate of tailoring steps. Kinetic studies of RED1 showed high affinity with ONBA, consistent with the requirement for an efficient reduction of a labile β-keto carboxylic acid. Interestingly, the methyl ester of ONBA acted as a competitive inhibitor of RED1, indicating the presence of strict substrate recognition toward the terminal acid functionality.

Actinorodin (ACT[1], **1**) is produced by one of the most genetically characterized bacteria, *Streptomyces coelicolor* A3(2) (*1*), and belongs to a class of aromatic antibiotics known as benzoisochromanequinones (BIQs). ACT was identified as a red pigment with weak bacteriostatic activity against *Staphylococus aureus* (*2*). Its unique structure with two naphthazarin rings connected by a direct C−C bond provides an indicator property under different pH conditions. This allows a simple complementation test of ACT production to be carried out in genetic analysis. It has become a favored model compound for the comprehensive study of antibiotic biosynthesis (*3*). Other BIQ examples are shown in Figure 1. The terminal carboxylate (C-1) is interconvertible with a γ-lactone formed with C-4. The carboxylate form includes ACT and nanaomycin A (**2**) (*4*) from *Streptomyces tanashiensis*, and the lactone form is represented by medermycin (MED, **3**) (*5*) from *Streptomyces* sp. K-73 and granaticin (GRA, **4**) (*6*) from *Streptomyces violaceoruber* Tü22. The BIQs all show a *trans* configuration with respect to the C-3 and C-15 chiral centers in either the type of (3*S*, 15*R*) or the type of (3*R*, 15*S*), implying strict stereochemical control during pyran ring formation. The existence of the lactone ring and the stereochemistry at C-3, -4, and -15 on the pyran ring are important elements for biological activity of the BIQs (*7*).

Cloning the ACT (*8*−*12*) biosynthetic gene cluster (the *act* cluster) gave rise to one of the first examples of type II polyketide synthases (PKSs) consisting of three functionally discrete proteins, keto-acylsynthase α (KSα), KSβ (chain length factor, CLF), and acyl carrier protein (ACP). The three components, designated as a minimal PKS, are widely

† This research was supported by MEXT. HAITEKU (2004-2008) and Grant-in-Aid for Scientific Research (C) (No. 17510184) to K. I.

* Corresponding author. Tel/Fax: +81-42-468-9184. E-mail: ichinose@musashino-u.ac.jp.

‡ The University of Tokyo.

§ Musashino University.

|| University of Bristol.

⊥ University of East Anglia.

[1] Abbreviations: ACT, actinorhodin; BIQ, benzoisochromanequinone; MED, medermycin; GRA, granaticin; PKS, polyketide synthase; KS, ketoacylsynthase; CLF, chain length factor; ACP, acyl carrier protein; KR, ketoreductase; ARO, aromatase; CYC, cyclase; DNPA, 4,10-dihydro-9-hydroxy-1-methyl-10-oxo-3*H*-naphtho[2,3-*c*]pyran-3-acetic acid; ONB-SNAC, *N*-acetyl cycteamine thioester of 3-oxo-4-naphthylbutyrate; ONBA, 3-oxo-4-naphthylbutyric acid; MONB, methyl 3-oxo-4-naphthylbutyrate; NPO, 1-(2-naphthyl)-propane-2-one; HNBA, 3-hydroxy-4-naphthylbutyric acid; OPB-SNAC, *N*-acetyl cysteamine thioester of 3-oxo-4-phenylbutyrate; OPBA, 3-oxo-4-phenylbutyric acid; HPBA, 3-hydroxy-4-phenylbutyric acid; AT, acyltransferase; DH, dehydratase; ER, enoyl reductase; TE, thioesterase; 3HAD, L-3-hydroxyacyl-CoA dehydrogenase.

10.1021/bi700190p CCC: $37.00
Published on Web 06/19/2007

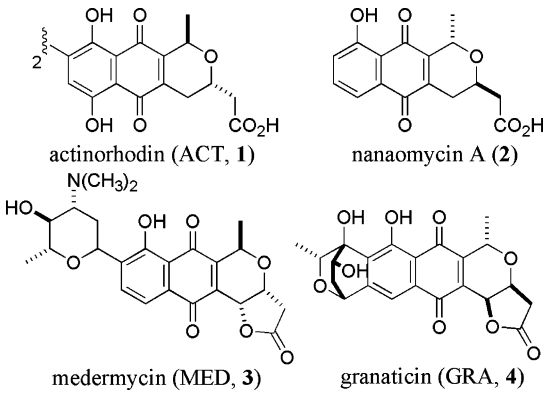

FIGURE 1: BIQ compounds produced by Streptomycetes.

distributed among PKSs related to aromatic polyketide biosynthesis (*3*). The three enzymes, ketoreductase (KR), aromatase (ARO: the *act*VII product), and cyclase (CYC: the *act*IV product) are closely associated with PKS, and their functions were neatly characterized by the *in vivo* recombinant systems using an *act* cluster-deficient strain of *S. coelicolor*, where recombinant sets of the genes of interest are selectively expressed on a suitable vector (*13*). The recombinants were further extended to the components of heterologous origin to demonstrate the feasibility of the PKS component to produce unnatural polyketide metabolites with a variety of chain length and cyclization patterns (*14*). The generally accepted procedure for the early stage of ACT biosynthesis is shown in Scheme 1. A linear octaketide produced by the **ACT** PKS is modified by the following reactions to produce the bicyclic intermediate (**5a**): reduction at C-9 by KR, with formation of the first ring; aromatization of the first ring by ARO; and second ring formation by CYC.

5a lies at the biosynthetic branch point toward various BIQ derivatives. The next step is stereospecific reduction at C-3 to afford either the 3*S*- or the 3*R*- configuration (*15*, *16*). In ACT biosynthesis, *act*VI-ORF1 was proven (*17*) to encode a dedicated reductase (RED1) to establish the (*S*)-configuration at C-3, by coexpression of *act*VI-ORF1 with the early ACT biosynthetic genes to produce 4,10-dihydro-9-hydroxy-1-methyl-10-oxo-3*H*-naphtho[2,3-*c*]pyran-3-(*S*)-acetic acid, (*S*)-DNPA (**6**), previously shown to be an ACT biosynthetic intermediate (*18*). **5a** cannot be isolated from any *act* mutants because of its spontaneous formation to the shunt anthraquinone products, DMAC (**7**) and aloesaponarin II (**8**). Further biochemical study of RED1 such as *in vitro* characterization requires a suitable analogous substrate. A series of unnatural β-keto-esters were subjected to biotransformations using *S. coelicolor* strain (CH999/pIJ5675) carrying combinations of ketoreducatase genes (*19*). Enantioselective reductions occurred in the recombinant strain carrying RED1. The closest structural analogue gave the (*S*) product in a highly enantiopure form, rigorously confirming that the *act*VI-ORF1 protein functions as stereospecific reductase at C-3 in ACT biosynthesis. In this study, the analogous substrates were all prepared as *N*-acetyl cysteamine thioesters, which are commonly used biochemical equivalents to the enzyme-bound form of **5a** (Scheme 1).

Although an ACP serves as an anchor of nascent intermediates during chain elongation in the type II PKS complex, it remains unknown when an ACP-free intermediate is released from the complex to post-PKS modification ("tailoring") steps. RED1 might recognize a carboxylic acid form (**5b**) of substrate to produce the first isolable ACP-free intermediate, **6**. However, accumulation of aloesaponarin II in a RED1 mutant indicates the labile property of an ACP-free intermediate to undergo terminal decarboxylation, suggesting that an intermediate may need to be properly bound with the ACP prior to the C-3 reduction to afford **6**. Thus, enzymatic characterization of RED1, particularly its substrate recognition, should provide some critical information on the interface between ACP-bound and unbound stages in the multienzymatic steps in ACT biosynthesis. In the present study, recombinant RED1 was purified to homogeneity followed by biochemical investigation to reveal its substrate recognition and catalytic mechanism.

MATERIALS AND METHODS

General Instrumentation. PCR was carried out using PTC-100 Programmable Thermal Controller (MJ Research, Inc.) with Phusion DNA polymerase (New England Biolabs) using the following step program: 98 °C, 30 s; (98 °C, 30 s; 68 °C, 10 s; 72 °C, 30 s) × 30 cycles; 72 °C, 5 min. Sequence analysis was performed on an automated DNA sequencer, PRISM-3100 (ABI). Protein samples were analyzed by SDS−PAGE on a Mini-Protean 3 system (Bio-Rad) and by gel-staining with GelCode Blue Stain Reagent (Pierce). Analytical and preparative HPLC were carried out on a TOSOH 8020 system. Column chromatography was performed using Wakogel C-200, and TLC was conducted on a 0.25 mm precoated silica gel plate (60GF_{254}, Merck). NMR spectra were obtained at 500 MHz (^{1}H) and 125 MHz (^{13}C) with a JEOL ECA-500 spectrometer, and the data were recorded as chemical shifts. Samples for LC/MS analysis were subjected to HP1100 series (Agilent Technologies)/LCQ system (Thermo Electron Co. Ltd.). Optical rotation was determined on a JASCO P-1010 digital polarimeter.

Materials. Solvents and chemicals were purchased from Wako Chemicals Ltd. (Tokyo), unless noted otherwise. *Escherichia coli* BL21-CodonPlus(DE3)-RIPL strain and pET-21a(+) were from Novagen. Standard DNA engineering experiments were performed using the *E. coli* DH5α strain. Ni Sepharose 6 Fast Flow resin and Superdex200 10/30 GL column (10 i.d. × 300 mm) were purchased from GE Health Care Bioscience. The HPLC columns specified below were purchased as follows. TSK-gel and CHIRALCEL/CHIRALPAK specified below were obtained from Tosoh Co. Ltd. and Daicel Chemical Industries Ltd., respectively. Oligonucleotide primers were obtained from Nihon Bioservice (Saitama, Japan).

Synthesis of Substrate Analogues and Reduced Products. Substrate analogues and their reduced products were synthesized as previously described (*19*). The key substances used in the experiments were prepared as follows. NMR data is available in the Supporting Information.

N-Acetyl Cysteamine. Potassium hydroxide pellets (13.7 g, 244.9 mmol) were added gradually to a solution of *N*,*S*-diacetyl cysteamine (12 g, 81.6 mmol) in distilled water (100 mL) at 0 °C. The reaction mixture was allowed to warm to room temperature and stirred for 3 h. 2 N HCl was added, and the mixture was extracted with dichloromethane (2× 100 mL). The combined organic extracts were dried over Na_2SO_4, and the solvent was removed *in vacuo* to give

Scheme 1: Proposed Biosynthetic Pathway of Actinorhodin in *S. coelicolor* A3(2), Consisting of Two Alternative Branches Involving Either a Bicyclic ACP-Bound (5a) or a Bicyclic ACP-Free (5b) Intermediate

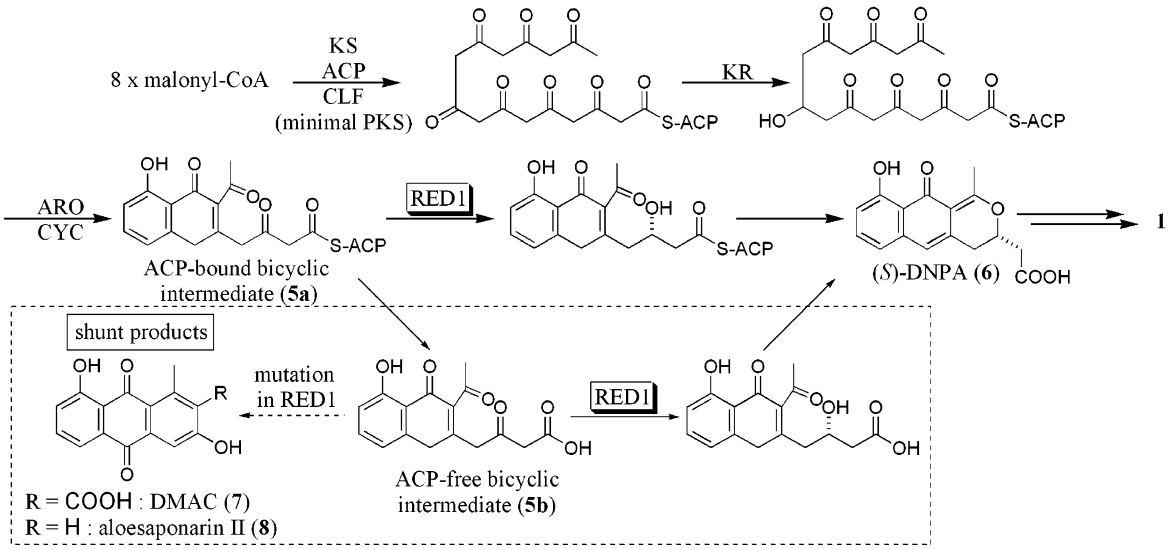

N-acetyl cysteamine (7.52 g, 63.7 mmol) as a colorless oil. *N*-acetyl cysteamine was dissolved in toluene and used in the following.

*N-Acetyl Cysteamine Thioester of 3-Oxo-4-naphthylbutyrate (ONB-SNAC) (**9a**)*. Oxalyl chloride (4.3 mL, 51.0 mmol) was added dropwise to a solution of 2-naphthylacetic acid (4.72 g, 25.4 mmol) in dry dichloromethane (40 mL) at 0 °C. The reaction was allowed to warm to room temperature and stirred for 16 h. The solvent was removed *in vacuo* to afford 2-naphthylacetyl chloride (5.12 g) as a yellow solid.

Pyridine (4.15 mL, 51.0 mmol) was added to a solution of Meldrum's acid (3.72 g, 25.4 mmol) in dichloromethane (20 mL) at 0 °C. To this was added dropwise a solution of 2-naphthylacetyl chloride (5.12 g, 25.0 mmol) in dichloromethane (20 mL). The reaction mixture was stirred at 0 °C for 1 h and at room temperature for 20 h. The resulting reaction mixture was washed with 2 N HCl (2× 40 mL), dried over $MgSO_4$, and concentrated *in vacuo* to give 1,3-dioxane-4,6-dione, 5-[1-hydroxy-2-(2-naphthalenyl)ethilidene]-2,2-dimethhyl-(9CI) (7.14 g) as a red solid.

A solution of *N*-acetylcysteamine in toluene (1 M, 25 mL) was added dropwise to a solution of 1,3-dioxane-4,6-dione, 5-[1-hydroxy-2-(2-naphthalenyl)ethylidene]-2,2-dimethyl-(9CI) (5.98 g, 19.2 mmol) in toluene (25 mL). The reaction mixture was heated under reflux for 7 h. The solvent was removed *in vacuo*, and the residue was dissolved in ethyl acetate (200 mL) and washed with H_2O (2× 100 mL). The ethyl acetate layer was dried over Na_2SO_4 and concentrated *in vacuo*. The residue was purified by silica gel column chromatography, eluting with 80% ethyl acetate/petroleum ether, and recrystallized from ethyl acetate/petroleum ether to afford the title compound **9a** (2.18 g, 32%) as a pale-yellow powder. MS: *m*/*z* 328.1 $[M - H]^-$ (APCI negative).

*3-Oxo-4-naphthylbutyric Acid (ONBA) (**9b**)*. Due to the labile property of β-keto acid, **9b** was prepared prior to enzymatic experiments by hydrolysis of **9c** (2.4 mg, 9.9 μmol) in H_2O (1 mL) with potassium hydroxide (250 μmol final concentration) under controlled conditions (30 °C, 2 h). The reaction mixture was neutralized with 1 N HCl and subjected to preparative HPLC with TSK-gel ODS-80T_M (7.8 i.d. × 300 mm; eluent, 40% aqueous acetonitrile containing 0.5% acetic acid; flow rate, 2.5 mL/min). Analytical HPLC of the purified sample indicates the presence of 99>% of **9b**. MS: *m*/*z* 227.4 $[M - H]^-$ (APCI negative).

*Methyl 3-Oxo-4-naphthylbutyrate (MONB) (**9c**)*. 1,3-Dioxane-4,6-dione, 5-[1-hydroxy-2-(2-naphthalenyl)ethylidene]-2,2-dimethyl-(9CI) (7.04 g, 22.6 mmol) was dissolved in anhydrous methanol (50 mL) and heated under reflux for 5 h. The solvent was removed *in vacuo*, and the residue was purified by silica gel column chromatography, eluting with 5% ethyl acetate/benzene and recrystallized from diethylether to afford **9c** (2.1 g, 34%) as colorless needles. MS: *m*/*z* 241.0 $[M - H]^-$ (APCI negative).

*1-(2-Naphthyl)-propane-2-one (NPO) (**9d**)*. Under essentially the same conditions as those used for the preparation of ONBA (**9b**), **9c** (30 mg, 92 μmol) was subjected to complete hydrolysis for 12 h, followed by decarboxylation. The reaction mixture was neutralized with 1 N HCl and extracted with EtOAc (10 mL). The extract was washed with H_2O, dried over Na_2SO_4, and concentrated *in vacuo*. The residue was purified by silica gel column chromatography eluting with benzene/acetone to give **9d** (5.4 mg, 29 μmol) as a pale-yellow solid.

*3-Hydroxy-4-naphthylbutyric Acid (HNBA) (**10**)*. Sodium borohydride (2.0 g, 52.63 mmol) was added in portions to a solution of methyl 3-oxo-4-naphtylbutyrate (MONB) (**9c**) (1.2 g, 4.96 mmol) in methanol (100 mL) at 0 °C. The reaction was stirred at 0 °C for 15 min and then at room temperature for 45 min. Water (50 mL) was added and the resulting solution extracted with chloroform (2× 150 mL). The combined organic extracts were washed with water (2× 50 mL) and brine (50 mL), dried over Na_2SO_4 and concentrated *in vacuo*. The residue was purified by silica gel column chromatography eluting with benzene/acetone (95/5) to afford methyl 3-hydroxy-4-naphthylbutyrate (210 mg) as a pale-yellow oil.

Potassium hydroxide (0.17 g, 3.00 mmol) was added to a solution of methyl 3-hydroxy-4-naphthylbutyrate (0.2 g, 0.82 mmol) in H_2O (30 mL), and the reaction mixture was stirred at room temperature for 4.5 h. The reaction mixture was acidified with 1 N HCl and extracted with chloroform (3×

50 mL). The combined organic extracts were washed with water (2× 20 mL) and brine (20 mL), dried over Na_2SO_4, and concentrated *in vacuo*. The resulting residue was purified by silica gel column chromatography, eluting with 50% petroleum ether/ethyl acetate to afford the racemic title compound (0.35 g, 56%) as a white solid. MS: *m*/*z* 229.3 $[M - H]^-$ (APCI negative).

N-Acetyl Cysteamine Thioester of 3-Oxo-4-phenylbutyrate (OPB-SNAC). Pyridine (10.5 mL, 129.3 mmol) was added dropwise to a solution of Meldrum's acid (9.3 g, 64.7 mmol) in dichloromethane (60 mL) at 0 °C. To this was added dropwise a solution of phenyl acetyl chloride (10 g, 64.7 mmol) in dichloromethane (60 mL). The reaction mixture was stirred at 0 °C for 1 h and at room temperature for 16 h. The resulting reaction mixture was washed with 2 N HCl (2× 60 mL), dried over Na_2SO_4, and concentrated *in vacuo* to give 1,3-dioxane-4,6-dione,2,2-dimethyl-5-(phenylacetyl)-(9CI) (15.67 g) as a red solid. This was dissolved in toluene (50 mL), and a solution of *N*-acetyl cysteamine in toluene (1.2 M, 50 mL) was added dropwise. The reaction mixture was heated under reflux for 6 h. The solvent was removed *in vacuo*, and the residue was dissolved in ethyl acetate (200 mL), washed with H_2O (2× 100 mL), dried over Na_2SO_4, and concentrated *in vacuo*. The crude residue was purified by silica gel column chromatography, eluting with 90% ethyl acetate/petroleum ether, and recrystallized from ethyl acetate/petroleum ether to afford the title compound (7.78 g, 43%) as pale-yellow crystals. MS: *m*/*z* 278.3 $[M - H]^-$ (APCI negative).

3-Oxo-4-phenylbutyric Acid (OPBA). Due to the labile property of a β-keto acid, OPBA was prepared prior to enzymatic experiments by hydrolysis of OPB-SNAC (5.3 mg, 19.1 μmol) in H_2O (1 mL) with potassium hydroxide (420 μmol final concentration) under controlled conditions (25 °C, 4 h). The reaction mixture was neutralized with 1 N HCl and subjected to preparative HPLC with TSK-gel ODS-80T_M (7.8 i.d. × 300 mm; eluent, 40% aqueous acetonitrile containing 0.5% acetic acid; flow rate, 2.5 mL/min). Analytical HPLC of the purified sample indicated the presence of 99>% of OPBA. MS: *m*/*z* 177.4 $[M - H]^-$ (APCI negative).

3-Hydroxy-4-phenylbutyric Acid (HPBA). 1,3-Dioxane-4,6-dione,2,2-dimethyl-5-(phenylacetyl)-(9CI) (12.0 g, 45.8 mmol) was dissolved in anhydrous methanol (100 mL) and heated under reflux for 6.5 h. The solvent was evaporated, and the residue was purified by silica gel column chromatography, eluting with benzene to afford methyl 3-oxo-4-phenylbutyrate (3.43 g) as a yellow oil.

Sodium borohydride (2.0 g, 52.63 mmol) was added to a solution of methyl 3-oxo-4-phenylbutyrate (2.0 g, 10.41 mmol) in methanol (100 mL), and the reaction mixture was stirred at 0 °C for 15 min and at room temperature for 45 min. The reaction was quenched by the addition of H_2O (100 mL) and extracted with chloroform (2× 150 mL). The combined organic extracts were washed with water (2× 50 mL) and brine (50 mL), dried over Na_2SO_4, and concentrated *in vacuo*. The crude residue was purified by silica gel column chromatography, eluting with chloroform to afford methyl 3-hydroxy-4-phenylbutyrate (0.47 g) as a pale-yellow oil.

Potassium hydroxide (0.60 g, 10.71 mmol) was added to a solution of methyl 3-hydroxy-4-phenylbutyrate (0.4 g, 0.82 mmol) in H_2O (50 mL), and the reaction mixture was stirred at room temperature for 1.5 h. The reaction mixture was acidified with 1 N HCl and extracted with chloroform (3× 50 mL). The combined organic extracts were washed with water (2× 50 mL) and brine (50 mL), dried over Na_2SO_4, and concentrated *in vacuo*. The crude residue was purified by silica gel column chromatography, eluting with benzene/acetone (80/20) to afford the racemic HPBA (0.08 g, 22%) as a white powder. MS: *m*/*z* 181.1 $[M + H]^+$ (ESI positive).

Plasmid Construction. To construct the plasmid, *act*VI-ORF1 was amplified from pIK402 (*19*) by PCR with the sense-primer, 5′-ACGTCGAGACATG**ATG**AGCACCGTGACAGTGAT-3′ (the underlined portion shows the *Nde*I site and the bold-faced portion the start codon), and the antisense-primer, 5′-TTCGAATTCAAG**CTT**GGTCTCCTCCTGGGGCT-3′ (underlined portion, *Hin*dIII site; bold-faced portion, stop codon) using the following step program: 98 °C, 30 s; (98 °C, 30 s; 68 °C, 10 s; 72 °C, 30 s) × 30 cycles; 72 °C, 5 min. The PCR products were gel-purified and digested with *Nde*I and *Hin*dIII followed by dephosphorylation. The resultant fragment was subcloned to the *Nde*I-*Hin*dIII sites of pET-21a(+) to give pIK611 (sequence checked).

Purification of Histidine-Tagged RED1. All purification procedures were carried out at 4 °C. *E. coli* BL21-CodonPlus-(DE3)-RIPL transformed with pIK611 was cultured at 37 °C, 220 rpm for 7 h in LB, and then 1 mL of the culture was transferred to 200 mL of LB and cultured at 30 °C, 220 rpm for 12 h without induction. The cells were harvested by centrifugation (5,000*g* for 10 min) and were suspended in 50 mM sodium phosphate buffer (containing 300 mM NaCl, 20% glycerol, and 30 mM imidazole at pH 7.8). After sonication, the soluble fraction was obtained by centrifugation (20,000*g* for 15 min). This fraction was applied to the Ni Sepharose 6 Fast Flow column, incubated for 12 h, and then eluted with 500 mM imidazole. The eluate was purified by gel filtration column chromatography on a Superdex200 10/30 GL column equilibrated with 50 mM sodium phosphate buffer (containing 150 mM NaCl and 15% ethyleneglycol at pH 7.8). From 800 mL of culture, 0.4 mg of the purified recombinant RED1 was obtained with 5% recovery of activity.

Quantitative Determination of β-Keto Acids. Due to their labile properties, the concentration of β-keto acids (ONBA and OPBA) used in the experiments was estimated by complete reaction with an excess amount of RED1. The reaction mixture was at 1 mL of final volume containing 100 mM sodium phosphate buffer (pH 6.5), 100 μM NADPH, 100 μL of β-keto acid, whose concentration was unknown, and 50 μM RED1. After incubation for 10 min, the reaction mixture was directly subjected to HPLC, and the concentration of ONBA or OPBA was estimated on the basis of the concentration of HNBA or HPBA using absorbance at 275 or 254 nm, respectively.

Structural Determination of Enzymatic Products from Substrate Analogues. Reactions were performed *in vitro* in a volume of 0.5 mL with sodium phosphate buffer (100 mM, pH 7.5) containing 100 μM NADPH, 25 μL of substrate analogue, and 35 nM of the enzyme solution. After incubation at 37 °C for 10 min, 25 μL of the reaction mixture was directly analyzed by reversed-phase HPLC under the following conditions: column, TSK gel ODS-80T_M (4.6 i.d. × 150 mm); column temperature, 40 °C; gradient, 10−95% (v/v) aqueous acetonitrile containing 0.5% AcOH within 30 min; flow rate, 1.0 mL/min; detection, absorption between

250 and 600 nm using a photodiode array detector. Then, reaction products were purified by preparative HPLC using TSK-gel ODS-80T_M (7.8 i.d. × 300 mm) under isocratic eluting conditions: 40% aqueous acetonitrile containing 0.5% AcOH, column temperature, 40 °C; flow rate, 2.0 mL/min. Each structure was determined by ^{1}H- and ^{13}C NMR spectroscopy. For enzymatic HNBA, its methyl ester was subjected to NMR analysis. Methyl ester of enzymatic HNBA: MS: *m*/*z* 243.4 $[M - H]^-$ (APCI negative), $[\alpha]_D$ +37.5 (*c* 1.12 × 10^{-4} $CHCl_3$). Enzymatic HPBA: MS: *m*/*z* 181.1 $[M + H]^+$ (ESI positive) $[\alpha]_D$ +6.17 (*c* 6.16 × 10^{-4} $CHCl_3$).

Kinetic Studies for RED1. All of the enzymatic assays were performed in a volume of 1 mL with sodium phosphate buffer (100 mM, pH 6.5). Typical activity was detected in reaction mixtures in a 1 cm light path cuvette containing 100 μM NADPH, 40 μM substrate analogue, and 50 μL of the enzyme solution. The decrease of A_{340} was monitored at room temperature. Reaction velocities were calculated on the basis of the A_{340} molar absorption coefficient of NADPH ($\epsilon = 6.21 \times 10^3$ M^{-1} cm^{-1}).

Chiral HPLC Analysis for Enzymatic Products. After *in vitro* reaction, the reaction products were extracted with ethyl acetate and purified by preparative HPLC. The purified products were analyzed by chiral HPLC under the following conditions: for HNBA, CHIRALCEL OD-RH (4.6 i.d × 150 mm), 27 °C, 25% aqueous acetonitrile containing 22.5 mM ammonium acetate at pH 3.6, and 1.0 mL/min; for HPBA, CHIRALPAK AD-RH (4.6 × 150 mm), 27 °C, 12.5% aqueous acetonitrile containing 26.25 mM ammonium acetate at pH 3.6, and 1.0 mL/min.

RESULTS

Purification of Recombinant RED1. RED1-encoding *act*VI-ORF1 has a composition of 924 bp corresponding 307 amino acids. Out of a number of trials with combinations of expression vectors and host (*Escherichia coli*) strains, a C-terminus His-tagged vector, pET-21a(+), and a host BL21-CodonPlus(DE3)-RIPL were chosen. Recombinant RED1 has an extra 12 amino acids, the deduced size being 34.7 kDa. Induction with IPTG was not needed to efficiently express active RED1, and proteins in the cell-free mixture were purified using a Ni Sepharose 6 Fast Flow column followed by Superdex 200 gel-filtration column chromatography to afford pure recombinant RED1. Purified RED1 showed a single band on SDS−PAGE at the deduced monomer size as shown in Figure 2A, and its native form was estimated to be a homodimer based on the elution profile (data not shown) of gel filtration chromatography.

Identification of Reaction Products. In place of a proposed bicyclic intermediate (**5a**), which is too unstable to be obtained, synthetic analogues were used as substrates. The *N*-acetylcysteamine thioester of 3-oxo-4-naphthylbutyrate (ONB-SNAC, **9a**) was synthesized essentially as described previously (*19*). 3-Oxo-4-naphthylbutyric acid (ONBA, **9b**), methyl 3-oxo-4-naphthylbutyrate (MONB, **9c)**, and 1-(2-naphthyl)-propan-2-one (NPO, **9d**) were derived from the Meldrum's acid derivative of **9c**. A fixed amount (3.2 pmol) of RED1 was used for an *in vitro* reaction mixture (0.5 mL) consisting of 12.5 nmol of a substrate and 50 nmol of NADPH. Reactivity was estimated by HPLC quantification

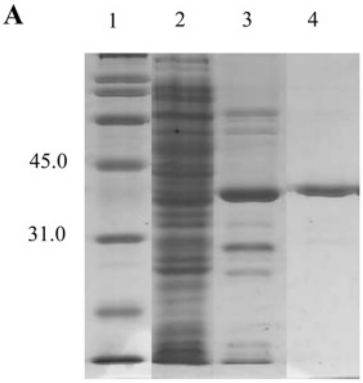

B

Purification step	Volume	Protein	Total activity	Specific activity	Recovery
	ml	*mg*	*units*	*units/mg*	*%*
Crude extract	40	96.3	128,600	1,300	100
Ni-Sepharose 6 Fast Flow	2	2.4	36,000	14,800	28
Superdex 200	1	0.42	6,800	16,000	5

FIGURE 2: Purification of RED1. (A) SDS−PAGE analysis of RED1 purification fraction. Lane 1, molecular weight marker; lane 2, crude extract; lane 3, Ni Sepharose 6 Fast Flow; lane 4, Superdex 200. The size of calculated recombinant RED1 is 37.4 kDa. (B) Purification table of RED1. One unit of enzyme activity was defined as the amount of this enzyme required to reduce 5 nmol of ONBA per 1 min at room temperature for 5 min in the reaction mixture.

of the reduced product, 3-hydroxy-4-naphthylbutylic acid (HNBA, **10**). Reactions with **9a** and **9b** produced **10**, whereas **9c** and **9d** were not reduced by RED1 (Figure 3A). HPLC profiles of reaction mixtures with **9a** and **9b** are shown in Figure 3B. When **9b** was used as a substrate, **9b** was completely reduced to **10** without any byproducts. However, the trial with **9a** failed to go to completion, and a substantial amount of **9a** remained. The productivity of **10** was only 6.5% compared with that of the reaction with **9b**. Importantly, no reduction of the NAC thioester itself occurred. The much more efficient reduction of the β-keto acid form (**9b**) compared to that of the SNAC form (**9a**) triggered us to test a monocyclic β-keto acid, 3-oxo-4-phenylbutyric acid (OPBA), as a substrate, and its complete reduction to 3-hydroxy-4-phenylbutyric acid (HPBA) was observed as expected (data not shown). These products were purified on a preparative scale, and their structures were confirmed by ^{1}H and ^{13}C NMR.

Optimization of Assay Conditions. To further characterize RED1 catalytic activity, assay conditions were optimized. In the presence of 50 nM RED1 and 100 μM NADPH, reactions were performed at room temperature for 5 min using ONBA at various concentrations. Measurement of the absorbance at 340 nm and product quantification by direct injection of reaction mixture to HPLC provided the conditions where the stoichiometric relationship holds between the consumption of NADPH and the production of HNBA. The working concentration of ONBA was subsequently determined to be 40 μM. Protein concentration dependence of RED1 activity was investigated over the range 2−32 nM (Figure 4). For the following kinetic studies, a protein concentration between 2 and 4 nM RED1 was used because HNBA was reduced by RED1 in a linear concentration-

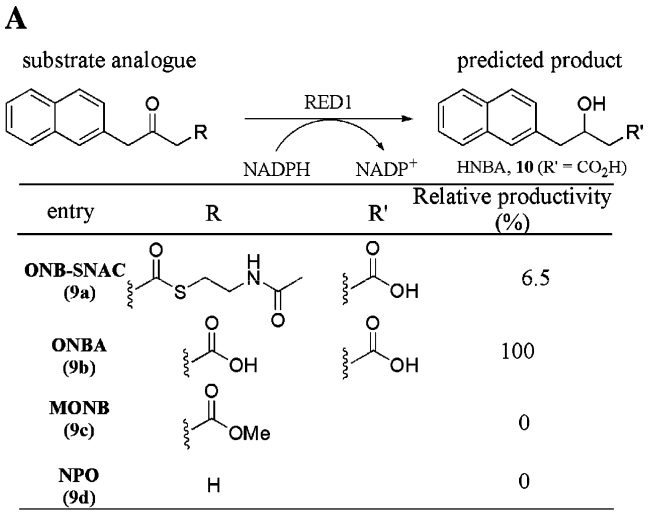

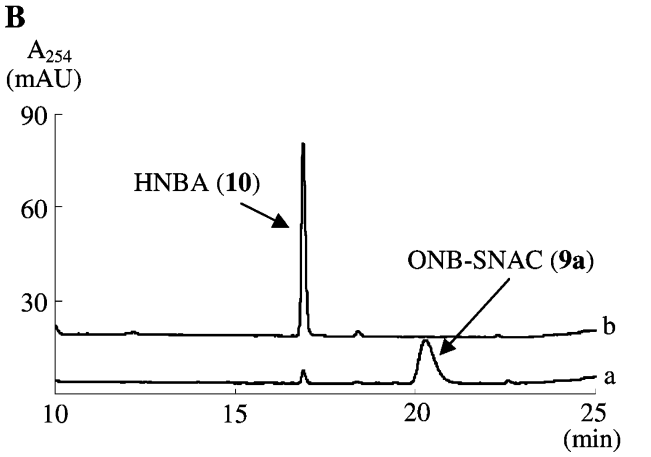

FIGURE 3: Reaction of RED1 *in vitro* with substrate analogues. (A) Structures of substrate analogues and relative velocity. (B) HPLC analysis of reaction mixture with ONB-SNAC or ONBA. Detection was by absorbance at 254 nm. The reaction of (a) ONB-SNAC or (b) ONBA with RED1 produced HNBA. The peaks at retention times of 16.6 and 20.1 min are HNBA and ONB-SNAC, respectively.

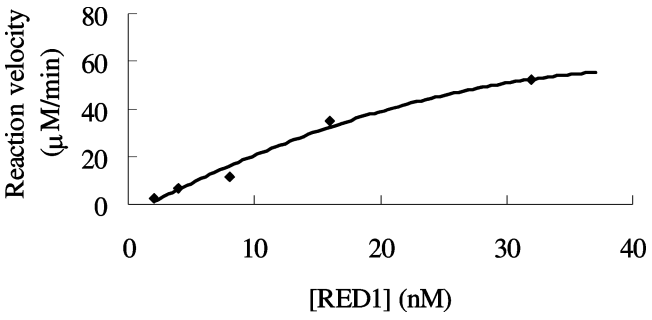

FIGURE 4: Reaction time course at various RED1 concentrations. Disappearance of NADPH was monitored at 2, 4, 8, 16, and 32 nM RED1.

dependent manner in this range (Supporting Information). The optimum assay conditions were thus established, and the purification table for RED1 (Figure 2B) is based on the activities estimated under these conditions.

Substrate Specificity. The productivity of HNBA (**10**) from ONB-SNAC (**9a**) with RED1 was only 6.5% compared with that from ONBA (**9b**). Measurements of reaction velocity using RED1 at concentrations from 2 to 128 μM under the standard assay conditions with **9a** demonstrated that the

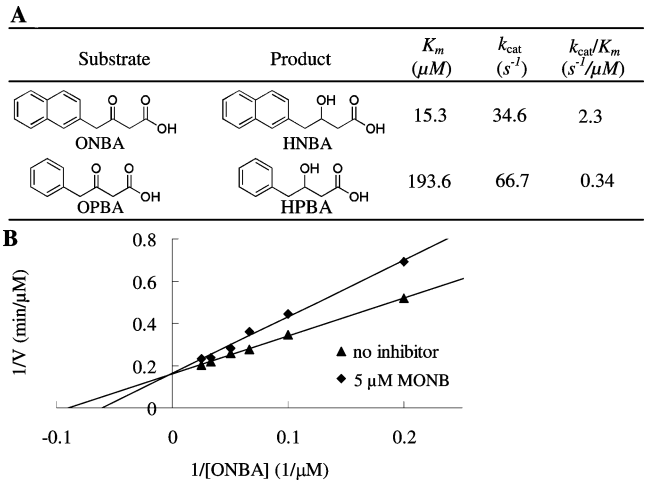

FIGURE 5: Kinetic study for RED1. (A) Kinetic parameters of RED1 for ONBA and OPBA. (B) Inhibition by MONB in the reduction of ONBA. Double reciprocal plots (a) with and (b) without MONB addition.

increase of reaction velocity was not observed at more than 4 μM of RED1, suggesting the presence of a rate-limiting step in the reaction course. At the concentration of 3.2 μM RED1, the reaction velocity was found to be seven times higher at pH 7.5 than at pH 6.5. Incubation of **9a** in assay mixtures without RED1 led to the production of **9b**, which was generated by nonenzymatic hydrolysis of **9a**. The nonenzymatic production of **9b** was seven times higher at pH 7.5 than at pH 6.5. These results crucially indicate that RED1 reduces the β-keto-group of the free acid form and not of the SNAC ester.

Kinetic Analysis of RED1 and Enzymatic Characterizations. RED1 reaction velocities were determined at RED1 concentrations of 3.2 μM (for ONBA) and 7 μM (for OPBA) under the standard assay conditions with varied concentrations of ONBA (4−40 μM) and OPBA (50−250 μM), respectively. From the Hanes−Woolf plot of these data, K_m and k_{cat} values for ONBA and OPBA were determined to be 15.3 μM and 34.6 s^{-1}, 193.6 μM and 66.7 s^{-1}, respectively. MONB did NOT react with RED1 but turned out to be a competitive inhibitor in the reduction of ONBA. (Figure 5). Some biochemical characterizations (Supporting Information) were also carried out for RED1 using ONBA (**9b**) at the optimum pH 6.5 with the temperature for the maximum reaction velocity at 35 °C. NADPH is a preferred cofactor over NADH (reaction velocity is 30 times less than that of NADPH).

Chiral HPLC Analysis of Enzymatic Products. Enzymatically produced HNBA and HPBA were subjected to chiral HPLC analysis. Racemic HNBA and HPBA showed two peaks at retention times of 14.4 and 15.7 min, and 10.3 and 11.7 min, respectively. Enzymatically produced HNBA and HPBA gave a single peak at retention times of 15.7 and 10.3 min, respectively (Figure 6). Therefore RED1 reduces both of ONBA and OPBA in a completely stereospecific manner (>99% *ee*).

DISCUSSION

Two subtypes of bacterial PKSs are involved in the formation of basic carbon backbones of antibiotics of polyketide origin. Type I PKSs are multifunctional large

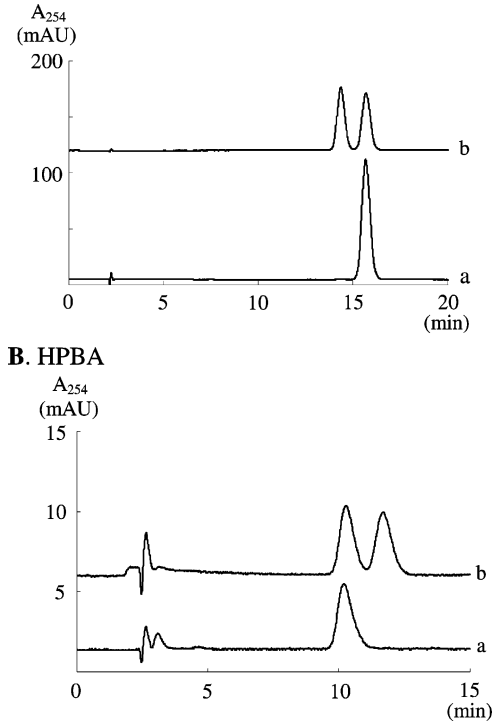

FIGURE 6: Chiral HPLC analysis for enzymatic products. (A) HNBA; (a) enzymatic HNBA and (b) racemic HNBA. (B) HPBA; (a) enzymatic HPBA and (b) racemic HPBA.

proteins consisting of functional modules arranged according to the order and number of necessary biosynthetic steps. One of the most extensively studied examples is the type I (*ery*) PKS involved in erythromycin biosynthesis in *Saccharopolyspora erythraea* (*20*). The *ery* PKS catalyzes six sequential condensations of one unit of propionyl CoA and six units of methylmalonyl CoA to afford 6-deoxyerythronolide B, which is the first enzyme-free macrolide intermediate. Analysis of the synthase revealed six domains each of KS, AT (acyltransferase), and ACP, allowing their separate functions for each chain-extension cycle. Apart from the three essential domains, there is a set of additional domains appropriate for each extension cycle, KR, dehydratase (DH), and enoyl reductase (ER) for facilitating six functional modules. Typically, such PKS assembly lines have a thioesterase (TE) domain at the C-terminal end of the last module, which hydrolyzes the processed polyketide chain to release products such as 6-deoxyerythronolide B. Type II PKSs function in an iterative way until a suitable number of condensations are completed. A nascent polyketide chain is apparently bound with an ACP in the subsequent cyclization steps. In contrast with type I, no dedicated TE was found in any of the known type II PKS biosynthetic gene clusters. An unsolved problem has been the timing of when a type II polyketide intermediate is released from the PKS complex for further structural modifications by post-PKS tailoring enzymes.

RED1 involved in ACT (**1**) biosynthesis reduces the C-3 position of a proposed bicylic intermediate (**5**) to produce the first isolable biosynthetic intermediate, **6** (Scheme 1). The present study enabled biochemical characterization of the pure recombinant RED1. Gel-filtration analysis suggested the native RED1 protein to function as a homodimer, in good agreement with our structural modeling study of RED1 (*21*), where a reasonable homodimer model was constructed. We used L-3-hydroxyacyl-CoA dehydrogenase (3HAD) from human heart (*22*−*24*) as a homologous (43% similarity to RED1) template for modeling. This enzyme is essential to the β-oxidation of fatty acids and catalyzes the dehydration of L-3-hydroxyacyl-CoA, whose partial structure is similar to that of the reactive portion of a bicyclic intermediate (**5**). The predicted RED1 models with and without ligand (cofactor) (*21*) consist of N- and C-terminal domains, and a substrate is supposed to bind in the cleft between the two domains. In the case of 3HAD, the significant domain shift observed in the structures with and without ligands clearly suggested (*22*) that the N-terminal domain rotates inward toward the C-terminal domain when the substrate binds. Occurrence of a similar domain shift in RED1 is very likely because of our previous successful biotransformations of various substrates (*19*).

Our enzymatic studies using analogous substrates demonstrated that a true substrate is most likely to be in the free acid form rather than in the ACP bound form. The SNAC-ester substrate (**9a**) was found to undergo hydrolysis to **9b** prior to the reduction. SNAC-ester substrates have widely been used as equivalents to enzyme-bound intermediates in biosynthetic studies. Our results strongly suggest that RED1 recognizes an enzyme-free bicyclic β-keto acid (**5b**) (Scheme 2). Kinetic study of RED1 revealed the K_m value for ONBA to be 15.3 μM, which is comparable to that (18.7 μM) (*23*) of 3HAD for acetoacetyl-CoA. Taking into account that **9b** is an analogous substrate, it is reasonable to speculate that the bicylic β-keto acid should provide the lower K_m expected from the obvious requirement of a labile β-keto acid to be efficiently reduced.

Interestingly, the methyl ester (**9c**) was found to be a competitive inhibitor of RED1, indicating a level of control in its substrate recognition. The identification of critical amino acid residues for recognition will require structural analysis of the ternary complex of RED1 with cofactor and substrate analogues. However, RED1 is rather tolerant to variations in the bicylic portion of substrates. On the basis of our finding, a series of β-keto acid substrates including ONBA (**9b**) and OPBA were subjected to the foregoing biotrans-

Scheme 2: Biosynthetic Pathway of Actinorhodin Proposed in This Study

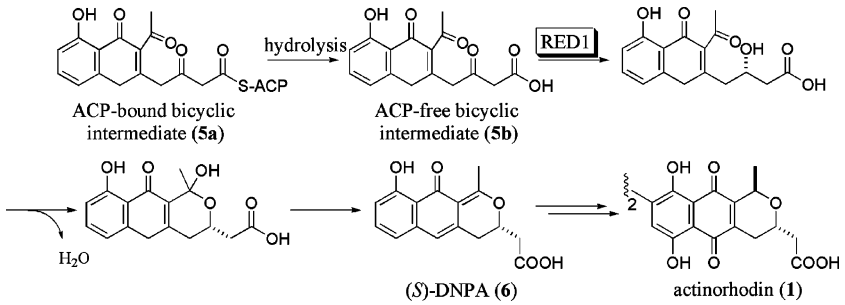

formation system (*19*) to demonstrate improved conversion yields and higher enantioselectivities (*25*). RED1 reductions of **9b** and OPBA *in vitro* gave enantiomerically pure compounds (Figure 6), demonstrating the feasibility of RED1 as a biocatalyst for the reduction of a wide range of β-keto acids without protection and with complete stereospecificity.

A reconstituted complex of the *act* minimal PKS efficiently produces the octaketide reaction products, SEK4 and SEK4b (*26*), implying that the intermediate could be released through additional TE activity of the *act* PKS after chain elongation. Further elaboration of a nascent polyketide chain in its producing type II PKS complex is also proposed by crystallographic analysis on the *act* KS-CLF heterodimer (*27*). However, our approach to understand the functional requirements of type II PKS is from the point of tailoring enzymes. Multienzymatic steps, leading to the production of an antibiotic, need to be based on the proper conveyance of intermediates from one enzyme to another. One possible explanation is that the β-keto acid (**5b**) (Scheme 2) could function as the first committed intermediate in an enzyme-unbound form. The present study also gives significant insight into the releasing point of an intermediate from the PKS complex involved in ACT biosynthesis.

ACKNOWLEDGMENT

We thank David A. Hopwood for the critical reading of this manuscript.

SUPPORTING INFORMATION AVAILABLE

Experimental data for biochemical characterizations of RED1 and NMR data for the compounds used for kinetic study. This material is available free of charge via the Internet at http://pubs.acs.org.

REFERENCES

1. Bentley, S. D., Chater, K. F., Hopwood, D. A., et al. (2002) Complete genome sequence of the model actinomycete *Streptomyces coelicolor* A3(2), *Nature 417*, 141−147.
2. Brockman, H., Pini, H., and Plotho, O. v. (1950) Actinomycete pigments. I. Actinorhodin, a red antibiotically active pigment from actinomycetes, *Chem. Ber. 83*, 161−167.
3. Hopwood, D. A. (1997) Genetic contributions to understanding polyketide synthase, *Chem. Rev. 97*, 2465−2497.
4. Ōmura, S., Tanaka, H., Koyama, Y., Oiwa, R., Takagiri, M., Awaya, J., Nagai, T., and Hata, T. (1974) Nanaomycins A and B, new antibiotics produced by a strain of *Strepomyces*, *J. Antibiot. 27*, 363−365.
5. Takano, S., Hasuda, K., Ito, A., Koide, Y., Ishii, F., Haneda, I., Chihara, S., and Koyama, Y. (1976) A new antibiotic, medermycin, *J. Antibiot. 29*, 765−768.
6. Corbaz, R., Ettlinger, L., Gaumann, E., Kalvoda, J., Keller-Schierlein, W., Kradolfer, F., Manukian, B. K., Neipp, L., Prelog, V., Reusser, P., and Zšhner, H. (1957) Products of metabolism of actinomycetes. IX Granaticin, *Helv. Chim. Acta. 40*, 1262−1269.
7. Ōmura, S., Tsuzuki, K., Iwai, Y., Kishi, M., Watanabe, S., and Shimizu, H. (1985) Anticoccidial activity of frenolicin B and its derivatives, *J. Antibiot. 38*, 1447−1448.
8. Hallam, S. E., Malpartida, F., and Hopwood, D. A. (1988) Nucleotide sequence, transcription and deduced function of a gene involved in polyketide antibiotic synthesis in *Streptomyces coelicolor*, *Gene 74*, 305−320.
9. Fernàndez-Moreno, M. A., Caballero, J. L., and Hopwood, D. A., Malpartida, F. (1991) The *act* cluster contains regulatory and antibiotic export genes, direct targets for translational control by the *bldA* tRNA gene of streptomyces, *Cell 66*, 769−780.
10. Fernàndez-Moreno, M. A., Martinez, E., Boto, L., Hopwood, D. A., and Malpartida, F. (1992) Nucleotide sequence and deduced functions of a set of cotranscribed genes of *Streptomyces coelicolor* A3(2) including the polyketide synthase for the antibiotic actinorhodin, *J. Biol. Chem. 267*, 19278−19290.
11. Fernàndez-Moreno, M. A., Martinez, E., Caballero, J. L., Ichinose, K., Hopwood, D. A., and Malpartida, F. (1994) DNA sequence and functions of the *act*VI region of the actinorhodin biosynthetic gene cluster of *Streptomyces coelicolor* A3(2), *J. Biol. Chem. 269*, 24854−24863.
12. Caballero, J. L., Martinez, E., Malpartida, F., and Hopwood, D. A. (1991) Organisation and functions of the *act*VA region of the actinorhodin biosynthetic gene cluster of *Streptomyces coelicolor*, *Mol. Gen. Genet. 230*, 401−412.
13. McDaniel, R., Ebert-Khosla, S., Hopwood, D. A., and Khosla, C. (1993) Engineered biosynthesis of novel polyketides, *Science 262*, 1546−1550.
14. McDaniel, R., Ebert-Khosla, S., Hopwood, D. A., and Khosla, C. (1995) Rational design of aromatic polyketide natural products by recombinant assembly of enzymatic subunits, *Nature 375*, 549−554.
15. Taguchi, T., Ebizuka, Y., Hopwood, D. A., and Ichinose, K. (2001) A new mode of stereochemical control revealed by analysis of the biosynthesis of dihydrogranaticin in *Streptomyces violaceoruber* Tü22, *J. Am. Chem. Soc. 123*, 11376−11380.
16. Li, A., Itoh, T., Taguchi, T., Xiang, T., Ebizuka, Y., and Ichinose, K. (2005) Functional studies on a ketoreductase gene from *Streptomyces* sp. AM-7161 to control the stereochemistry in medermycin biosynthesis, *Bioorg. Med. Chem. 13*, 6856−6863.
17. Ichinose, K., Surti, C., Taguchi, T., Malpartida, F., Booker-Milburn, K. I., Stephenson, G. R., Ebizuka, Y., and Hopwood, D. A. (1999) Proof that the *act*VI genetic region of *Streptomyces coelicolor* A3(2) is involved in stereospecific pyran ring formation in the biosynthesis of actinorhodin, *Bioorg. Med. Chem. Lett. 9*, 395−400.
18. Cole, S. P., Rudd, B. A. M., Hopwood, D. A., Chang, C.-J., and Floss, H. G. (1987) Biosynthesis of the antibiotic actinorhodin analysis of blocked mutants of *Streptomyces coelicolor*, *J. Antibiot. 40*, 340−347.
19. Anson, C. E., Bibb, M. J., Booker-, Milburn, K. I., Clissold, C., Haley, P. J., Hopwood, D. A., Ichinose, K., Revill, W. P., Stephenson, G. R., and Surti, C. M. (2000) Genetic engineering of *Streptomyces coelicolor* A3(2) for the enantioselective reduction of unnatural β-keto-ester substrates, *Angew. Chem., Int. Ed. 39*, 224−227.
20. Saunton, J., and Weissman, K. (2001) Polyketide biosynthesis: a millennium review, *J. Nat. Prod. Rep. 18*, 380−416.
21. Taguchi, T., Kunieda, K., Takeda-Shitaka, M., Takaya, D., Kawano, N., Kimberley, M. R., Booker-Milburn, K. I., Stephenson, G. R., Umeyama, H., Ebizuka, Y., and Ichinose, K. (2004) Remarkably different structures and reaction mechanisms of ketoreductases for the opposite stereochemical control in the biosynthesis of BIQ antibiotics, *Bioorg. Med. Chem. 12*, 5917−5927.
22. Barycki, J. J., O'Brien, L. K., Strauss, A. W., and Banaszak, L. J. (2001) Glutamate 170 of human L-3-hydroxyacyl-CoA dehydrogenase is required for proper orientation of the catalytic histidine and structural integrity of the enzyme, *J. Biol. Chem. 276*, 36718−36726.
23. Barycki, J. J., O'Brien, L. K., Bratt, J. M., Zhang, R., Sanixhvili, R., Strauss, A. W., and Banaszak, L. J. (1999) Biochemical characterization and crystal structure determination of human heart short chain L-3-hydroxyacyl-CoA dehydrogenase provide insights into catalytic mechanism, *Biochemistry 38*, 5786−5798.
24. Barycki, J. J., O'Brien, L. K., Strauss, A. W., and Banaszak, L. J. (2000) Sequestration of the active site by interdomain shifting. Crystallographic and spectroscopic evidence for distinct conformations of L-3-hydroxyacyl-CoA dehydrogenase, *J. Biol. Chem. 275*, 27186−27196.
25. Booker-Milburn, K. I., Kimberley, M. R., Gillan, R., Taguchi, T., Ichinose, K., Stephenson, G. R., Ebizuka, Y., and Hopwood, D. A. (2005) Enantioselective reduction of β-keto acids with engineered *Streptomyces coelicolor*, *Angew. Chem., Int. Ed. 44*, 1121−1125.
26. Dreier, J., Shah, A. N., and Khosla, C. (1999) Kinetic analysis of the actinorhodin aromatic polyketide synthase, *J. Biol. Chem. 35*, 25108−25112.
27. Keatinge-Clay, A., Maltby, D. A., Medihradszky, K. F., Khosla, C., and Stround, R. M. (2004) An antibiotic factory caught in action. *Nat. Struct. Mol. Biol. 11*, 888−893.

BI700190P